

Chicken Prion Tandem Repeats Form a Stable, Protease-Resistant Domain<sup>†</sup>

Edward M. Marcotte and David Eisenberg\*

UCLA–DOE Laboratory of Structural Biology and Molecular Medicine, Department of Chemistry and Biochemistry, University of California, Los Angeles, Los Angeles, California 90095-1569

Received June 23, 1998; Revised Manuscript Received November 6, 1998

**ABSTRACT:** Prion-linked diseases, such as mad cow disease, scrapie, and the human genetic disorder Creutzfeldt–Jakob disease, are fatal neurodegenerative diseases correlated with changes in the secondary structure of neural prion protein. We expressed recombinant chicken prion protein in *Escherichia coli* and purified the protein to homogeneity. Circular dichroism spectra of the 26 kDa recombinant protein closely resemble those of prion protein purified directly from healthy hamster brain. The chicken prion protein exists as a soluble, monodisperse monomer but can be forced to multimerize following lyophilization and resuspension. We analyzed the chicken prion protein domain structure by proteolysis and show that, unlike the mammalian homologues, the chicken prion protein N-terminal tandem amino acid repeats form a stable, protease-resistant domain. This domain probably represents a physiologically functional unit. As tested by both mass spectrometry and circular dichroism, the mature chicken prion protein does not bind copper, unlike synthetic peptides from the chicken prion N-terminus, suggesting that binding copper is not the physiological activity of the chicken prion. However, copper strongly destabilizes the prion protein and depresses the melting temperature by 30 °C, presumably by binding to the unfolded form of the prion protein. The chicken prion N-terminus may have evolved to fold without a cofactor, unlike mammalian prion proteins, whose N-termini are disordered without cofactors such as copper present. Chicken prion offers an alternative to intractable mammalian prions for structural studies of the amino-terminal domain.

The “prion hypothesis” holds that an aberrant conformation of a normal cellular protein is the essential, perhaps sole, component of the infectious agent responsible for several fatal neurodegenerative diseases, among these bovine spongiform encephalopathy (BSE, known as “mad cow disease”), sheep spongiform encephalopathy (“scrapie”), and the human genetic disease Creutzfeldt–Jakob disease (CJD). Prion diseases received widespread attention in the recent epidemic of mad cow disease in Great Britain, with over 160 000 confirmed cases in the past decade (World Animal Health Organization figures). Fears that mad cow disease could be transmitted to humans led the British government to order the destruction of over 2 188 000 head of cattle (UK Ministry of Agriculture, Fisheries, and Food figures as of March 1998).

Although it is not certain that the prion protein is the disease’s causative agent, it is the primary component of infectious brain fractions (1, 2), and infection occurs only in hosts expressing the prion protein (3). In the course of disease (4, 5), the normal 28 kDa<sup>1</sup> cellular prion protein

(PrP<sup>C</sup>) is converted into a form with modified secondary structure (PrP<sup>Sc</sup>, named for the sheep prion disease scrapie). No change in covalent modification has been detected in PrP<sup>Sc</sup>; instead, it shows significantly enhanced protease resistance and decreased solubility as compared to PrP<sup>C</sup>. While PrP<sup>C</sup> is entirely degraded by proteinase K, PrP<sup>Sc</sup> is degraded into a stable fragment consisting of amino acids 90–231 (hamster numbering, 1). The converted prion protein may then be incorporated into a growing aggregate, forming amyloid-like plaques in infected brains (6–8).

Little is known about the normal cellular role of the prion protein. In hamster, the 209 amino acid protein is processed from a 254 amino acid precursor and is tethered by a covalently attached glycosylphosphatidylinositol anchor (GPI; 9) to the outer leaflet of neuronal plasma membranes. Although no enzymatic activity is associated with the protein, both in vivo results with mammalian prion proteins (10) and studies of synthetic peptides (11–13) have shown that prion protein can bind copper ions at an N-terminal site containing a series of tandem eight amino acid repeats. To date, copper binding is the only biochemical function associated with the prion protein. Knockout mice show disrupted circadian rhythms (14), loss of Purkinje cells (15), and abnormalities in long-term potentiation (16). Such evidence suggests that the prion protein is required for normal neural function, although its exact role is unclear.

Lack of enough pure prion protein, especially in unmodified or homogeneously modified form, has hindered detailed biochemical analysis. Purification from brain is difficult, and yields are low [e.g., 230 µg of PrP<sup>C</sup> from 450 mg of hamster brain by Pergami et al. (17)]. Although recombinant systems

<sup>†</sup> This work was supported in part by grants from the NIH and DOE and by an appointment of E.M.M. to the Alexander Hollaender Distinguished Postdoctoral Fellowship, sponsored by the U.S. Department of Energy and the Oak Ridge Institute for Science and Education.

\* To whom correspondence should be addressed.

<sup>1</sup> Abbreviations: PrP, prion protein; ChPrP, chicken prion protein; ChPrPH6, chicken prion protein fused to a carboxy-terminal hexahistidine sequence; GhPrP, golden hamster prion protein; mPrP, mouse prion protein; PrP<sup>C</sup>, cellular form of prion protein; PrP<sup>Sc</sup>, scrapie form of prion protein; SDS, sodium dodecyl sulfate; PAGE, polyacrylamide gel electrophoresis; PMSF, phenylmethylsulfonyl fluoride; CD, circular dichroism; GST, glutathione *S*-transferase; MBP, maltose binding protein; H6, hexa-histidine; kDa, kilodalton(s); PBS, phosphate-buffered saline.

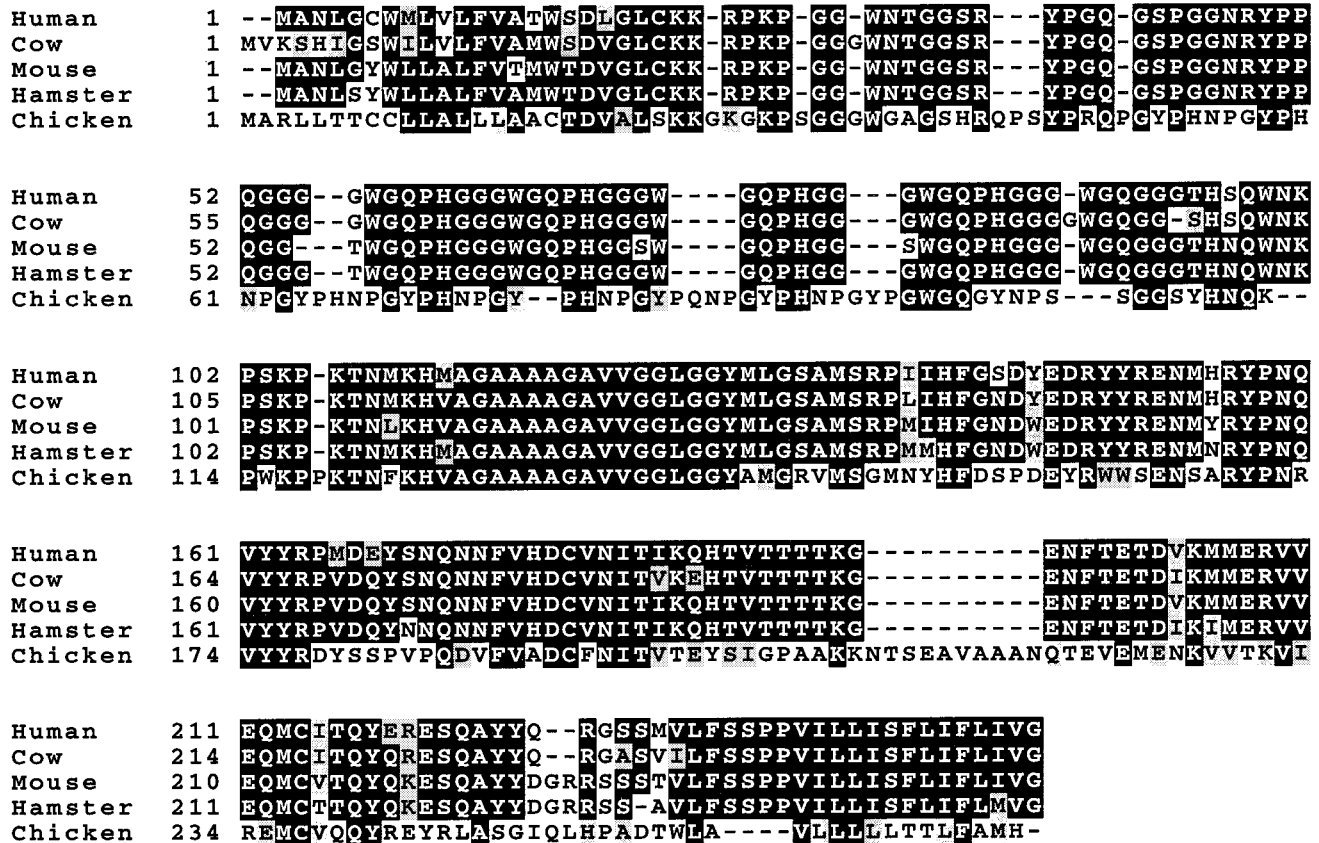


FIGURE 1: Multiple sequence alignment of prion proteins. Chicken prion protein has amino-terminal tandem repeats distinct from those of mammalian prion proteins. Significantly higher similarity is seen in residues 106–207 (chicken numbering) of the prions. Residues are shaded black when more than half in a column are identical; gray shading indicates homologous residues.

have been developed, these often produce insoluble prion protein which must be refolded (18, 19). Currently, the only assay available to monitor proper folding is circular dichroism.

Because of such difficulties in obtaining protein and assaying activity, chicken prion protein is an important control for studying the general properties of prion proteins and presents an alternative to the difficult mammalian proteins. The chicken prion is the most divergent protein in an otherwise highly homologous protein family (23), sharing 44% identity with the human prion amino acid sequence. By contrast, hamster prion is 93% identical to human. The differences between chicken and mammalian prions should help verify the generality of the more curious aspects of prion proteins—for example, the apparent complete lack of structure in the mammalian amino-terminal tandem amino acid repeats (20, 21). Conservation of these properties in chicken prion protein would suggest that they have an essential role in prion protein function.

So far, chicken prion protein is the only nonmammalian prion protein whose gene has been isolated (22). The chicken gene is expressed in chicken spinal chord and brains; the protein made is strongly homologous to mammalian prion proteins in the central region (see Figure 1), but diverges widely in the amino terminus and contains inserts in the carboxy terminus. The essential features of mammalian prions are conserved: (1) an amino-terminal signal sequence that is removed in the mature protein; (2) a stretch of basic residues; (3) tandem amino acid repeats [(PHGGGWGQ)<sub>6</sub> in mammals, (PHNPGY)<sub>8</sub> in chicken] followed by (4) a

highly conserved core, and by (5) a carboxy-terminal signal that is removed when the mature protein is linked to GPI. Both chicken and mammalian prions are multiply *N*-glycosylated (22, 24).

Although much elegant work has been done on the cell biology of the chicken prion protein (25, 26), little is known about how the mammalian and chicken prion proteins compare biochemically. Here, we present the expression, purification, and characterization of recombinant chicken prion protein, describe its multimerization *in vitro* and lack of copper binding, and describe the presence, unique to the avian prion protein, of a protease-resistant domain composed of the amino-terminal tandem repeats.

## MATERIALS AND METHODS

**Cloning.** Seven recombinant chicken prion protein expression plasmids were created from a cDNA clone of chicken prion kindly provided by Glenn Telling and Stanley Prusiner of the University of California at San Francisco. Plasmids were designed to express either glutathione *S*-transferase (GST), maltose binding protein (MBP), or a hexahistidine sequence (H6) fused to either the mature chicken prion protein sequence (residues 24–249 of the full-length chicken prion) or an amino-terminal fragment (residues 24–103) containing the basic patch and tandem repeats. Ser 24 would have been removed in normal cellular prion processing to produce a protein beginning at Lys 25, but we included Ser 24 to avoid expressing a recombinant protein beginning with lysine, which is disfavored at *E. coli* protein amino termini [see review by Georgiou (27)].

The chicken prion gene was amplified by PCR and cloned into expression vectors as follows: For GST fusions, the chicken prion gene was cloned into the *EcoRI* and *BamHI* restriction sites of parent vector pGEX-2T (Pharmacia). For MBP fusions, the gene was cloned into the *EcoRI/BamHI* sites of parent vectors pMAL-P2 and pMAL-C2 (New England BioLabs). Cloning into the *NdeI* and *XhoI* sites of plasmid pET20b+ (Novagen) produced carboxy-terminal H6 fusions with a two amino acid linker (LE). The proper construction of all expression plasmids was verified by DNA sequencing.

**Protein Expression and Purification.** pET20b-based plasmids were transformed into *E. coli* BL21 (DE3) and BLR (DE3) cells (Novagen) for protein expression. pGEX-2T and pMAL-based vectors were transformed into INV $\alpha$ F' and TOP10 cells (Invitrogen) for protein expression. Typically, cells were grown in 2 $\times$  YT media with ampicillin at 37 °C, induced at 0.5 OD<sub>600 nm</sub> with addition of 0.1–1 mM IPTG, and harvested after 4 h. Cell pellets were washed with 50 mM Tris-HCl, pH 8, lysed, and centrifuged at 38000g to separate soluble from insoluble cell fractions.

GST fusion proteins were purified as per Pharmacia protocols. GST fusion proteins were separated from GST (produced intracellularly from proteolytic cleavage of GST fusion proteins) by passage over a strong cation exchange column (Pharmacia HiTrap SP column) in 50 mM Tris-HCl, pH 7.4. GST eluted in the flow-through fraction, GST fusion protein eluted with 520 mM sodium chloride, and a heterodimer of GST with GST fusion protein eluted with 420 mM sodium chloride.

**Refolding of ChPrPH6.** Mature chicken prion with a carboxy-terminal hexa-histidine sequence (designated ChPrPH6) was expressed only in the insoluble cell fraction and was refolded using the following protocol: The insoluble cell fraction from 1 L of cells was washed successively with 25 mL of 100 mM Tris-HCl, pH 8, with 25 mL of 100 mM Tris-HCl, pH 8, 0.5% Tergitol NP-40, and with 25 mL of 1 M sodium chloride. The pellet from the salt wash was resuspended by sonication in 2 mL of 6.5 M guanidine hydrochloride, 100 mM Tris-HCl, pH 7.4. After pelleting insoluble material, the now soluble, denatured chicken prion was refolded by rapidly diluting 1:50 into 1.3 M urea, 100 mM Tris-HCl, pH 7.4, 100 mM glycine, 100  $\mu$ M oxidized glutathione, 1 mM reduced glutathione, 100  $\mu$ M PMSF. This solution was stirred for an hour at room temperature, and then at 4 °C overnight. Precipitate was centrifuged out and then resuspended in guanidine hydrochloride for another cycle of denaturing/refolding. Roughly equivalent yields of soluble ChPrPH6 were found in three successive cycles of denaturing/refolding, but yields dropped at the fourth round, suggesting that only 20–30% of the ChPrPH6 available in the first round refolded properly in each round. The soluble, refolded protein from each round was applied to a Pharmacia HiTrap chelating column charged with nickel sulfate. ChPrPH6 of very high purity was eluted with a linear gradient of 50–500 mM imidazole in 20 mM Na HEPES, pH 7.8, 300 mM sodium chloride. For general analyses, ChPrPH6 was exchanged by dialysis into 5 mM Na HEPES, pH 7.8. For amino acid analysis, ChPrPH6 was exchanged into 10 mM ammonium acetate, pH 6.8, and analyzed by Pico-Tag chemistry using a precolumn reaction with phenyl isothiocyanate.

**Characterization of ChPrPH6.** Circular dichroism was performed with an AVIV CD Spectrometer Model 62A DS. Each spectrum is an average of 20 scans of 0.84 mg/mL ChPrPH6 in 5 mM Na HEPES, pH 7.8, with buffer background similarly measured and subtracted. Spectra of ChPrPH6 at pH 5.5 were collected on 55  $\mu$ g/mL ChPrPH6 in 5 mM sodium acetate buffer. For testing copper binding, CuCl<sub>2</sub> was added to the above conditions in a broad range of concentrations (0.2  $\mu$ M to 1.2 mM), diluting the sample by less than 2%. The CD spectra were smoothed with three-point sliding window averaging. Protein concentration determination for molar ellipticity calculations came from amino acid analysis determination of the UV absorption extinction coefficient  $\epsilon$  (280 nm, 1 mg/mL) = 2.63. CD spectra were fit with coil, helix, and strand content using the neural network program k2d (28).

Melting temperature was measured by monitoring the circular dichroism ellipticity at 222 nm of 3 mL of 55  $\mu$ g/mL ChPrPH6 in 5 mM Na HEPES, pH 7.8, while raising the sample temperature from 5 to 95 °C. Changes in melting temperature due to copper were measured using identical conditions supplemented with 80  $\mu$ M CuCl<sub>2</sub> (approximately 40-fold molar excess).

Dynamic light scattering measurements were performed on 1 mg/mL ChPrPH6 protein in 5 mM Na HEPES, pH 7.8, on a Protein Solutions dp801 instrument using chicken egg white lysozyme (2.5 mg/mL in PBS) and pig pancreas trypsin (1 mg/mL in 5 mM Na HEPES, pH 7.8) as standards.

For mass spectrometry, 1 mg/mL protein in 5 mM Na HEPES, pH 7.8, was deposited with twice the volume of 10 mg/mL sinapinic acid in 70% acetonitrile, 0.1% trifluoroacetate onto a sample plate and analyzed by matrix-assisted laser desorption/ionization mass spectrometry with a time-of-flight detector (MALDI-TOF). Copper binding was assayed by first incubating 74  $\mu$ M ChPrPH6 with 20 mM CuCl<sub>2</sub> (270-fold molar excess) for 1 h at 4 °C, and then analyzing as above. Products of protease digestions were monitored by running proteolytic reactions in the above buffer, stopping proteolysis by addition of 10 mM PMSF, and analyzing the products by SDS-PAGE and by MALDI-TOF as described for intact protein. For the 6.6 kDa proteinase K-generated fragment, the matrix  $\alpha$ -cinnamic acid was used to suppress overlap of peaks from multiply charged proteinase K molecules.

**Proteolysis of ChPrPH6.** Protease digestions were performed using either pig pancreatic trypsin or *T. album* proteinase K in 5 mM Na HEPES, pH 7.8. Protease preparations contained 1–5% calcium acetate. Typically, 12  $\mu$ g of ChPrPH6 was mixed with 50 ng or 1  $\mu$ g of trypsin in a 6  $\mu$ L reaction and incubated at room temperature for 0–60 min. Proteolysis was stopped at various times by addition of SDS-PAGE gel loading buffer, and then boiling for 5 min. To test proteinase K sensitivity, 0.8 mg/mL ChPrPH6 was incubated with 20  $\mu$ g/mL proteinase K for 1 h at 37 °C or with 400  $\mu$ g/mL proteinase K for 1 h at room temperature. Proteolysis was stopped by addition of SDS-PAGE gel loading buffer and boiling for 5 min.

The amino-terminal sequence data and amino acid composition of the tryptic and proteinase K fragments were obtained from fragments separated on a 20% acrylamide SDS-PAGE gel and blotted onto an Immobilon P<sup>8Q</sup> membrane. Five to seven cycles of Edman degradation were

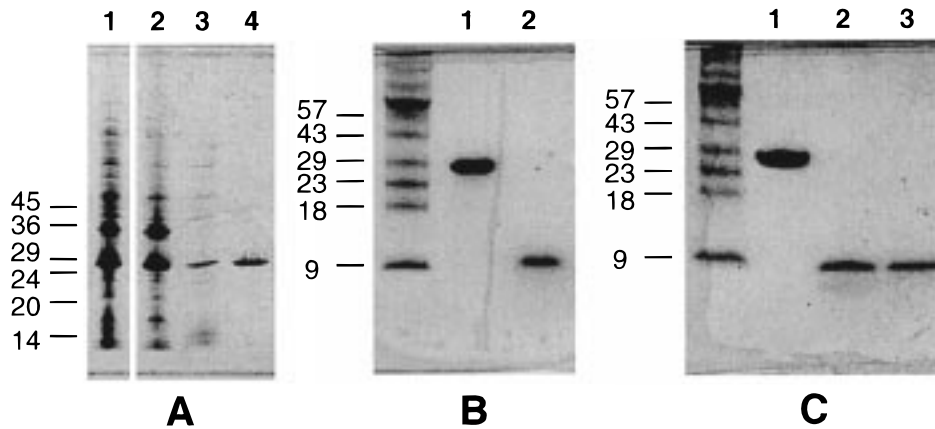


FIGURE 2: (A) Purification of the chicken prion protein ChPrPH6. Lane 1, 10–15% acrylamide gradient SDS–PAGE gel showing the insoluble cell fraction; lane 2, the inclusion body pellet after washing. Lane 3 shows protein refolded by rapid dilution of guanidine-denatured inclusion bodies, and lane 4 shows purified ChPrPH6 eluted from a nickel-charged chelating column. (B) Digestion of ChPrPH6 with trypsin. Lane 1 of the 20% acrylamide SDS–PAGE gel shows undigested ChPrPH6; lane 2 shows products of incubating 12  $\mu\text{g}$  of ChPrPH6 with 1  $\mu\text{g}$  of trypsin for 1 h, 24  $^{\circ}\text{C}$ . (C) 20% acrylamide SDS–PAGE gel showing proteinase K digestion of ChPrPH6. Lane 1, undigested ChPrPH6; lane 2, reaction products of incubating 4  $\mu\text{g}$  of ChPrPH6 with 20 ng of proteinase K at 37  $^{\circ}\text{C}$ , 1 h, or (lane 3) with 400 ng of proteinase K, 24  $^{\circ}\text{C}$ , 1 h.

performed on excised fragments in a gas-phase Porton/Beckman sequencer and analyzed by reverse-phase HPLC.

*Fragment Identification by Amino Acid Composition.* Approximate positions and lengths of fragments were obtained from amino acid composition analysis by maximizing the agreement between the measured amino acid composition and the amino acid composition in a window sliding along the known ChPrPH6 sequence. A score was calculated for each window position and window length:

$$\frac{\sum_{AA} (N_{\text{obs}} - N_{\text{calc}})^2}{L}$$

where  $N_{\text{obs}}$  is the number of amino acids of a given type observed experimentally,  $N_{\text{calc}}$  is the number of amino acids of a given type observed in the sliding window, and the sum is taken over the types of amino acids measured in the amino acid compositional analysis, and then normalized by dividing by window length  $L$ . Aspartate and asparagine were binned together, as were glutamate and glutamine, since they are measured together experimentally. Cysteine and tryptophan residues were not measured in the experimental analysis and were not included in the score calculation. The score approached a minimum when the highest agreement was reached between the experimental data and the amino acid sequence in the given window. Scores calculated as a function of window position or length were fit by seventh order polynomial regression using the program XMGR. Minimum scores were then taken from the calculated curve.

Analyses of data, including sliding window averaging, averaging of multiple experiments, analyses of mass spectra peaks, and fitting of amino acid composition data, were all performed in PERL scripts on a DEC Alpha workstation. Multiple sequence alignments were calculated by ClustalW (29) and formatted using BoxShade 3.21. NIH Image (Wayne Rasband, NIMH) was used to calculate intensity profiles from scanned gel images.

## RESULTS

*Cloning and Expression of Chicken Prion.* A hexahistidine fusion protein construct (pChPrPH6) produced

significant amounts of mature chicken prion protein (residues 24–249) that was easily purified and stable to further manipulation. In addition, an amino-terminal fragment (residues 24–103) of chicken prion protein could be solubly expressed as both glutathione *S*-transferase and maltose binding protein fusions. However, only the GST fusion protein (GXrpt) was expressed to high levels and could be affinity-purified. Binding of the MBP fusion proteins (C2rpt/P2rpt) to amylose resin was blocked by the presence of the fusion peptide; non-affinity-based purification was not pursued for these constructs. In all fusions to the amino-terminal prion protein domain, degradation of the fusion proteins was observed in purified protein and in soluble cell extracts. Proteolysis was not blocked by protease inhibitor cocktails or chelating agents such as EDTA or phenanthroline.

*Purification and Characterization of ChPrPH6.* The mature chicken prion/hexa-histidine fusion protein (ChPrPH6) was expressed in inclusion bodies, denatured, and refolded to form soluble ChPrPH6. Nickel affinity chromatography produced a monomeric, stable, extremely pure preparation (>98% by Coomassie-stained SDS–PAGE and mass spectrometry) of recombinant chicken prion protein (see Figure 2A). Amino acid composition analysis and mass spectrometry (Figure 3) verified the proper molecular mass (25 886 Da) and composition of ChPrPH6. Amino-terminal sequencing confirmed proper removal of the initial methionine, giving the sequence SKKGK... The mass of ChPrPH6 was measured by electrospray/ionization mass spectrometry as  $25\,890.9 \pm 3.7$  Da, matching the molecular mass with the initial methionine removed. Mass measured by MALDI-TOF ( $25\,943 \pm 26$   $m/z$ ) exceeded the calculated molecular mass, probably due to the presence of two sodium adducts, as spectra were collected from protein in 5 mM Na HEPES buffer. The mass spectrum revealed a double peak, suggesting that most of the ChPrPH6 has had the amino-terminal methionine properly removed, although protein approximately one residue shorter ( $25\,767 \pm 26$   $m/z$ ) is also present.

Unlike prion protein purified from chicken brain (22), the recombinant chicken prion is not derivatized with glycosylphosphatidylinositol, nor is it glycosylated. However, far-

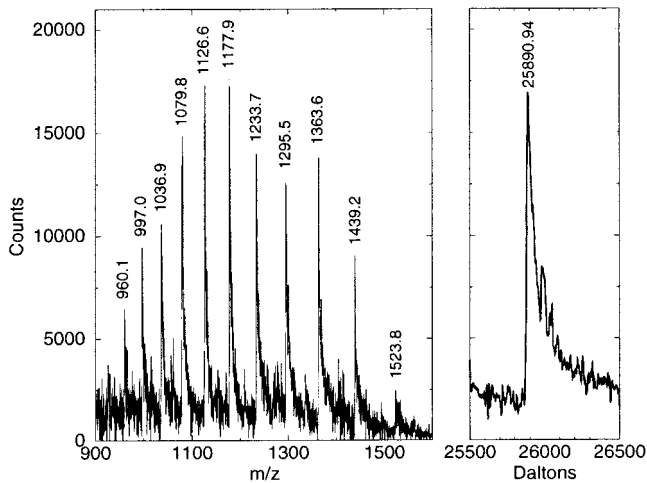


FIGURE 3: Mass spectrum of purified ChPrPH6 protein (1.0 mg/mL in  $\text{dH}_2\text{O}$ ). Raw electrospray/ionization mass spectra in the left window show peaks corresponding to monomer plus 27 protons (labeled 960.1  $m/z$ ) to 17 protons (labeled 1523.8  $m/z$ ). In the right window, a transform of the raw data shows the ChPrPH6 mass is  $25\,890.94 \pm 3.7$  Da.

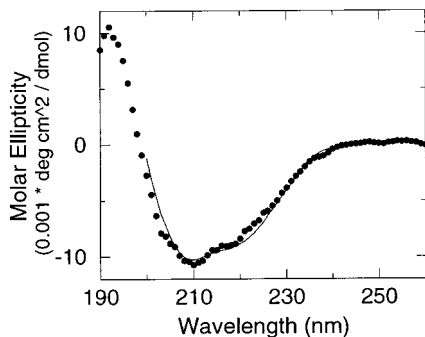


FIGURE 4: Circular dichroism spectrum (average of 20 spectra) of ChPrPH6 in 5 mM Na HEPES, pH 7.8, is shown as filled circles. The best fit of data between 200 and 240 nm by the neural network program k2d is shown as a solid line.

UV CD spectra of the recombinant chicken prion protein (Figure 4) closely resemble the CD spectra of prion protein purified directly from hamster brain [e.g., see Figure 3 of Pan et al. (4)], implying that the recombinant chicken prion resembles the native form of the hamster prion protein.

**Oligomeric State of ChPrPH6.** ChPrPH6 runs as a single band on native PAGE, migrating alongside monomeric recombinant hamster prion protein (amino acids 23–231; supplied by Darlene Groth and Stanley Prusiner). Estimation of molecular mass by dynamic light scattering (Table 1) shows that ChPrPH6 exists as a monodisperse 26–28 kDa monomer in solution. Even when these data are artificially fit with a bimodal regression, 97% of the mass is fit as 31 kDa and 3% as only 57 Da.

However, a ChPrPH6 multimer is observed after lyophilizing 5  $\mu\text{L}$  of 1 mg/mL ChPrPH6 from 5 mM Na HEPES, pH 8, and resuspending in deionized water (reproducing the prelyophilization buffer conditions, as Na HEPES is non-volatile). Following lyophilization and resuspension, a second band appears on native PAGE (see Figure 5) in 17% yield, as determined by scanning densitometry. The putative multimer migrates 49% of the distance migrated by the native ChPrPH6, suggesting a molecular mass 3 times the molecular mass of the native ChPrPH6 if the charge-to-mass ratio is

perfectly maintained. As it is expected that oligomerization perturbs the charge-to-mass ratio, the exact multimeric state is difficult to estimate from native PAGE alone. Introducing 10% error in migration distance measurements due to charge variation gives a molecular mass estimate for the multimer 2.5–3.9 times the monomeric molecular mass. The higher molecular mass ChPrPH6 band appeared spontaneously in 2.4 mg/mL ChPrPH6 preparations stored at 4  $^\circ\text{C}$  for over 100 days.

**Copper Binding.** ChPrPH6 mixed with 270-fold molar excess of  $\text{CuCl}_2$  1 h before analysis by MALDI-TOF mass spectrometry showed no shift in  $m/z$  values and gave an indistinguishable spectrum from ChPrPH6 alone. Incubation with 100 mM EDTA prior to mass spectrometry resulted in a reduction of  $m/z$  values by 43 daltons, probably attributable to loss of sodium adducts (46 Da per 2 sodium atoms), although potassium (39 Da) and calcium (40 Da) are also possible. No change in the CD spectrum shape occurred while titrating in  $\text{CuCl}_2$  to ChPrPH6, although at  $\text{CuCl}_2$  concentrations above 80  $\mu\text{M}$ , ChPrPH6 began to form fibrous precipitates. Loss of ChPrPH6 from solution was observed as an overall decrease in observed ellipticity (see Figure 6A,B). The change in ChPrPH6 concentration due to dilution with  $\text{CuCl}_2$  was less than 2%, although the decrease in peak ellipticity at 210 nm was 21% in 80  $\mu\text{M}$   $\text{CuCl}_2$ . Scaling of the curves to compensate for the decreasing concentration of soluble protein revealed no significant changes in CD spectra due to the presence of copper at either pH 5.5 or pH 7.8 (see Figure 6C). To test if copper destabilized the prion protein, the melting temperature of ChPrPH6 was measured with and without copper present (Figure 7). Native protein was found to have a melting temperature at 72  $^\circ\text{C}$  and did not denature reversibly. Addition of 80  $\mu\text{M}$   $\text{CuCl}_2$  depressed the melting temperature to 42  $^\circ\text{C}$ .

**Proteolysis of ChPrPH6.** Digest of ChPrPH6 with either trypsin or proteinase K produces fragments stable to further proteolysis. A tryptic digest time course (data not shown) indicates that ChPrPH6 is degraded through several metastable intermediates, including a 13 kDa fragment, before a 9 kDa domain is produced that is stable even to high levels of trypsin (see Figure 2B). Analysis of the tryptic digest by mass spectrometry (see Figure 8) reveals that the dominant tryptic fragment has a molecular mass of  $8871.3 \pm 8.9$  daltons. The tryptic fragment amino terminus is QPGYP... by amino-terminal sequencing, which unambiguously identifies Q49 of the full-length chicken prion sequence as the amino terminus of the fragment. Taking the sequencing and mass spectroscopy data together suggests that the 9 kDa fragment extends from amino acid 49 to amino acid 129 of the full-length chicken prion protein, a fragment of 8849 Da as calculated from the sequence. Amino acid compositional analysis supports these data (see Figure 9), with the maximum agreement between experimental amino acid composition and calculated amino acid composition occurring in a fragment 79 amino acids long beginning at amino acid Q49 of the mature chicken prion.

Although proteinase K generated a 9 kDa fragment clearly visible by SDS–PAGE (Figure 2C), a mass peak for the 9 kDa fragment was not visible by MALDI-TOF using either sinapinic acid or  $\alpha$ -cinnamic acid as matrixes. Amino-terminal sequencing of the SDS–PAGE-resolved fragment identified the amino terminus as (GS)(H)RQPSYPR, where

Table 1: Dynamic Light Scattering Shows That Recombinant Chicken Prion Exists as a Monodisperse 26 kDa Monomer in Solution

protein	translational diffusion coefficient ( $\times 10^{-13}$ m <sup>2</sup> /s)	average hydrodynamic radius (nm)	polydispersity (nm) <sup>a</sup>	measured mass (daltons)	predicted mass (daltons)
lysozyme	1135	1.7	0.781	12000	14313
trypsin	920	2.2	0.858	21000	24409
ChPrPH6	852–866	2.4–2.5	<0.4 (monodisperse)	26000–28000	25886

<sup>a</sup> Polydispersity is calculated as the standard deviation of the hydrodynamic radius about the average radius.

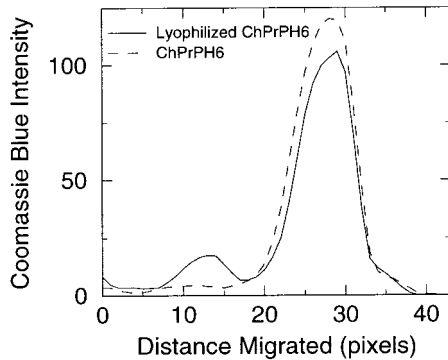


FIGURE 5: Scanned intensity profiles of lanes from a 20% acrylamide native gel electrophoresis experiment show the production of a higher molecular mass protein following lyophilization of ChPrPH6. Zero distance migrated represents the stacking gel/running gel interface. Coomassie Blue dye intensity is in arbitrary units scaled from 1 to 256.

(GS) and (H) are minor products contaminating the primary sequence. This unambiguously identifies the PK 9 kDa fragment amino terminus as Arg 42, with two alternative starts at Gly 39 and His 41. From agreement with amino acid composition analysis of the SDS–PAGE-resolved fragment (see Figure 9), the fragment length was computed as 72 amino acids, identifying the fragment as amino acids Arg 42 to approximately Lys 113 of the full-length chicken prion. The fragment would have a predicted molecular weight of 8002 Da, in agreement with the SDS–PAGE data.

Proteinase K digestion of ChPrPH6 also produces a minor fragment absent from the tryptic digest, estimated to be 6.6 kDa by SDS–PAGE (Figure 2C). Amino-terminal sequencing showed two fragments were present, HNQKPW... and SKKGKG..., identifying amino acids His 110 and Ser 24 as the fragment amino termini. Mass spectra show five peaks in the 6–7 kDa region, the largest at  $6739 \pm 7$   $m/z$  units (see Figure 10). The differences between peak positions (130–181  $m/z$  units) are consistent with single amino acid changes, suggesting that the carboxy-terminal ends of the 6.6 kDa fragments are ragged. Assigning fragments by closest agreement with  $m/z$  values suggests that one fragment extends from amino acid Ser 24 to Pro 80 (calculated mass of 6122 Da) and the other from His 110 to either Asn 166 or Pro 171 (calculated mass of 6278 and 6593 Da).

## DISCUSSION

We find the recombinant chicken prion ChPrPH6 to be a stable, ordered, soluble protein possessing secondary structure much like that observed in prion protein purified directly from hamster brain. This suggests that ChPrPH6 folds properly into the physiologically relevant form. Moderately high yields of protein (2.4 mg/L cells) can be obtained at extremely high purity (>98%), allowing sensitive tests of structure and searches for activity to be performed. In

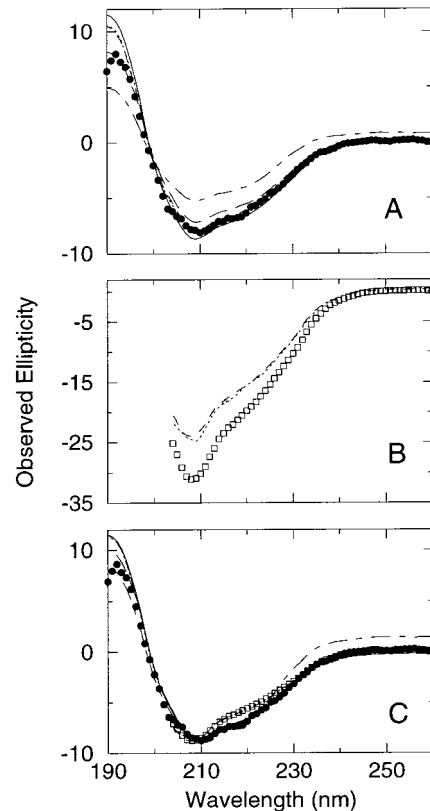


FIGURE 6: (A) Circular dichroism spectra of ChPrPH6 at pH 7.8 during titration with copper chloride. ChPrPH6 alone is shown as filled circles, while titrations of ChPrPH6 with copper(II) chloride from a parallel experiment are shown as lines. Curves represent ChPrPH6 with, from deepest to shallowest minima at 210 nm, 80  $\mu$ M CuCl<sub>2</sub>, 80  $\mu$ M CuCl<sub>2</sub> after 10 min at 25 °C, 80  $\mu$ M CuCl<sub>2</sub> after 25 min at 25 °C, 80  $\mu$ M CuCl<sub>2</sub> after 110 min at 37 °C, and 1.2 mM CuCl<sub>2</sub>. (B) Circular dichroism spectra of ChPrPH6 at pH 5.5 during titration with copper chloride. ChPrPH6 alone is represented as open squares. The two curves represent ChPrPH6 with 80  $\mu$ M CuCl<sub>2</sub> (dotted line) and 400  $\mu$ M CuCl<sub>2</sub> (dashed line). (C) Scaling of all circular dichroism spectra from the copper chloride titrations shows that the observed difference in spectra stems from depletion of soluble protein, not from copper-induced conformational change. Symbols are as in parts A and B.

contrast, fusion proteins of ChPrP or its amino-terminal domain were not useful.

**Oligomeric State.** Light scattering results and native gel analysis both indicate that ChPrPH6 exists solely as a monomer, within the detection limit of both systems. However, lyophilization has been used in other protein systems [e.g., with RNase A in Liu et al. (30)] to produce oligomers from monomeric proteins. In these systems, the combined effects of concentration and dehydration or acid pH induce one domain of a multidomain protein to exchange positions with the equivalent domain of another protein molecule, producing an oligomer. Likewise, when lyophilized, ChPrPH6 oligomerizes to a higher molecular mass

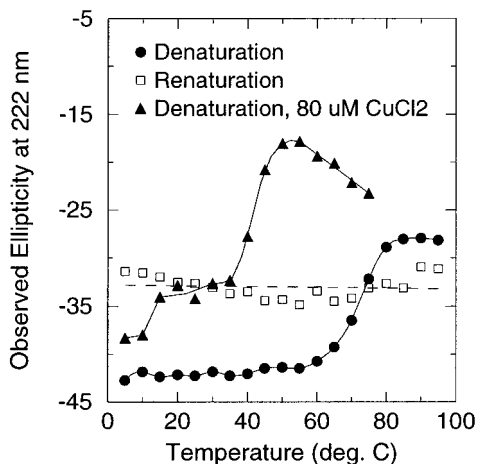


FIGURE 7: Melting temperature of ChPrPH6 in the absence and presence of copper obtained by measuring circular dichroism ellipticity at 222 nm while varying the temperature. The presence of 80  $\mu$ M copper chloride depresses the melting temperature of ChPrPH6 from 72 to 42  $^{\circ}$ C. (Denaturation data are fit with spline curves only to clarify the illustration.)

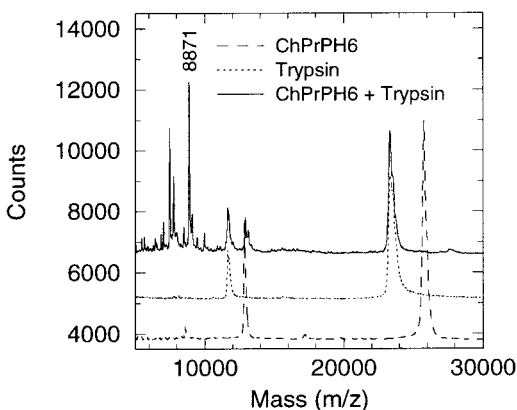


FIGURE 8: MALDI-TOF analysis of the products of a tryptic digest of ChPrPH6. 12  $\mu$ g of ChPrPH6 was incubated with 1  $\mu$ g of trypsin for 30 min at room temperature before stopping the reaction with PMSF and analyzing the products, shown as a solid line trace. For comparison, spectra of undigested ChPrPH6 (dashed line) and trypsin (dotted line) are shown. All detectable full-length ChPrPH6 is digested in the reaction. The primary trypsin digestion product is a fragment of  $8871 \pm 8.9$   $m/z$ . Two fragments of approximately 13 000  $m/z$  fragment are also visible in this spectrum; these are degraded at longer time points. Spectra are offset along the y axis for clarity of display.

species. The multimer molecular mass estimated from native PAGE is consistent with either a dimer, a trimer, or a tetramer. Whether this oligomerization is a model for pathological prion aggregation (31), represents a physiologically significant oligomerization, or is an intriguing artifact is not clear and remains for further study.

**Chicken Prion Secondary Structure.** In the far-UV circular dichroism analysis, the minima at 210 and 218 nm show that ChPrPH6 contains moderate  $\alpha$ -helical content. The secondary structure content was sensitive to pH; ChPrPH6 at pH 5.5 showed more random coil than at pH 7.8. Analysis of the chicken prion CD spectrum by the neural network program k2d (28) gives the distribution of secondary structures as 24%  $\alpha$  helix, 35%  $\beta$  sheet, and 41% random coil, with an estimated maximum mean error equal to 12.2%. (Maximum mean error =  $[\sum_{3\text{states}}(\text{actual percent secondary structure} - \text{predicted percent secondary structure})]/3$ . This

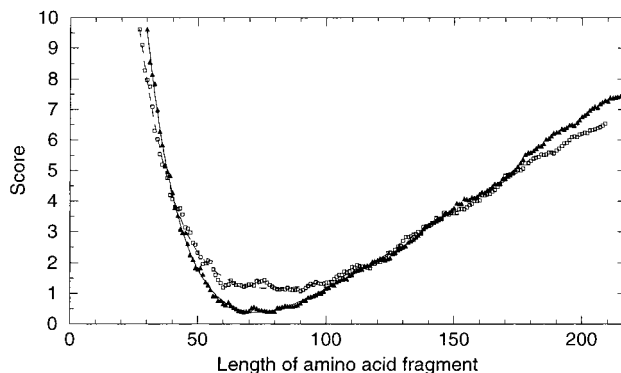


FIGURE 9: Prediction of proteolytic fragment carboxy termini by calculating the agreement between the experimentally determined amino acid composition and that calculated from a stretch of the known ChPrPH6 sequence. The fragment amino terminus was held fixed at either Q49 or R42, as determined by microsequencing of the 9 kDa tryptic and proteinase K fragments, respectively. The fragment length was varied and the agreement calculated as described under Materials and Methods section. Lowest scores, indicating maximal agreement, predict a 79 amino acid tryptic fragment and a 72 amino acid proteinase K fragment.

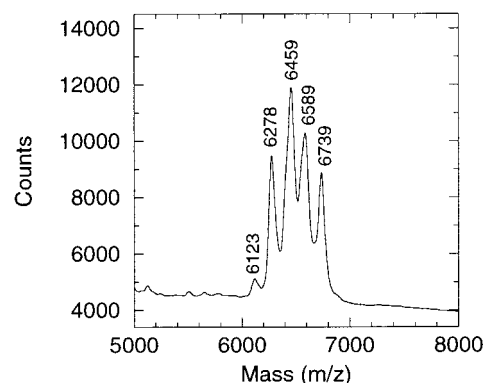


FIGURE 10: Expanded view of the mass spectrum of proteinase K-digested ChPrPH6 protein reveals the molecular masses of the 6.6 kDa fragments. The presence of five peaks indicates that the fragment ends are ragged, differing by about one amino acid in length for each successive peak.

large error, giving a broad range of values from 12% to 36%  $\alpha$  helix, stems from the dissimilarity of ChPrPH6 to the proteins in the k2d learning set.)

By comparison, PrP<sup>C</sup> was predicted from FTIR data to have 42% helix, and PrP<sup>Sc</sup> was predicted, also from FTIR, to have 30% helix (4), although these values probably have a similarly large error range. Therefore, the helical content of ChPrPH6 is compatible, within error, with either PrP<sup>C</sup> or PrP<sup>Sc</sup>.  $\beta$  sheet content, a significant criterion in distinguishing PrP<sup>C</sup> (at 3%) from PrP<sup>Sc</sup> [43%; (4)], is estimated in ChPrPH6 as being present at 23–47% of the structure. By this criterion, ChPrPH6 is intermediate in  $\beta$  sheet content, but closer to PrP<sup>Sc</sup>. The amino acid sequence of the chicken prion tandem repeats has no inherent tendency toward either helix or sheet and is predicted to form exposed loops by the secondary structure prediction program PHD (32). However, this is inconsistent with the protease resistance of this region, which implies a reasonably compact domain and not a set of exposed loops. Because the N-terminus is proline/glycine-rich and therefore also unlikely to be either  $\alpha$  helical or  $\beta$  strand in nature, we can expect that the three-state secondary structure predictions for prion proteins will probably contain significant errors.

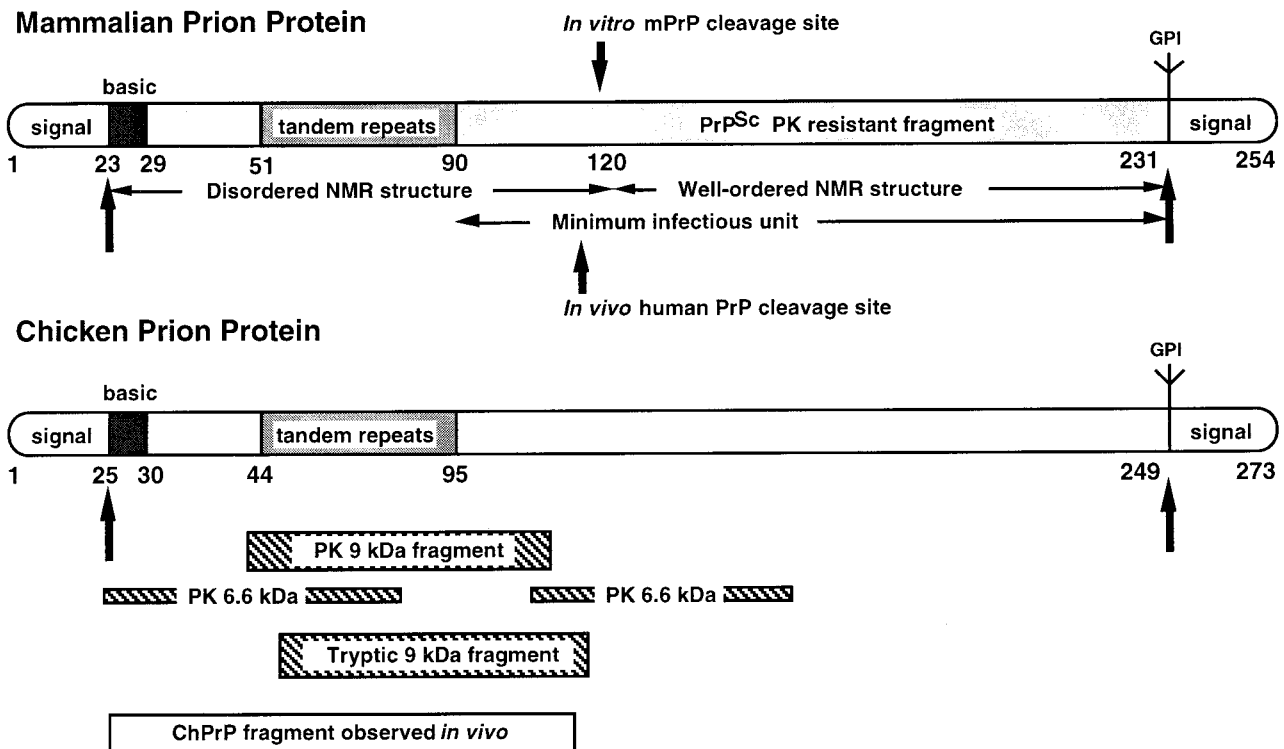


FIGURE 11: Diagram of protease cleavage patterns observed in prion proteins. Boldface arrows indicate sites of proteolytic cleavage. Fragments generated by proteolysis of ChPrPH6 are shown as hatched rectangles beneath the diagram of the chicken prion protein. Horizontal locations of fragments indicate relative position in the amino acid sequence. For comparison, the fragment released by *in vivo* proteolysis (25) is shown as an open rectangle.

Table 2: Comparison of Mammalian and Chicken Tandem Repeats, Presenting Evidence That Chicken Prion Tandem Repeats Form a Well-Folded, Reasonably Compact Domain

mammalian repeats (PHGGGWGQ) <sub>6</sub>	avian repeats (PHNPGY) <sub>8</sub>
<b>As Synthetic Peptides</b>	
bind copper, as measured by mass spectrometry (11) chromatography/atomic absorption (11) circular dichroism (12) fluorescence quenching (12) raman spectroscopy (13): random coil without copper $\alpha$ -helical with copper	bind copper, as measured by mass spectrometry (11) circular dichroism: (12) increase in random coil with copper fluorescence quenching (12)
<b>In Mature-Length Recombinant Protein</b>	
repeats are flexible and disordered, as measured by NMR (20, 21) proteinase K sensitivity (35)	repeats are not flexible, but are apparently constrained, as measured by proteinase K resistance (36) trypsin resistance (36) inability to bind copper on kinetic time scale (mass spectrometry, circular dichroism data) (36) depression of melting temperature by copper (36)
<b>In Vivo</b>	
repeats can be proteolytically removed and have not been observed extracellularly (33)	repeats are proteolytically removed, but remain detectable in the extracellular medium (25)

*Structure of Tandem Repeats.* It is clear from analyses of proteins and their structures that repeated amino acid sequences fold into repeated structural units. (Examples include collagen and the leucine-rich repeats of porcine ribonuclease inhibitor.) The mammalian prion repeats have been examined previously by NMR (20, 21) and found to be disordered. That this disorder is their native structure in the brain seems unlikely. An alternative explanation is that disorder arises from experimental conditions (that is, abnormal folding from inclusion bodies) or from lack of a cofactor normally present *in vivo*. From the data presented here, the chicken prion tandem repeats—clearly similar though sig-

nificantly diverged from mammalian repeats—have a structure compact enough to block access to potential protease cleavage sites.

The production of a 9 kDa ChPrPH6 fragment stable to further proteolysis is intriguing, as the chicken prion behaves differently from both cellular and scrapie-form mammalian PrP. These differences are illustrated in Figure 11. Mammalian PrP<sup>C</sup> is entirely degraded by proteinase K, and the ChPrPH6 fragment differs from that obtained by proteolysis of pathological hamster PrP<sup>Sc</sup> [producing the GhPrP fragment 90–231 (1)]. These data suggest that the chicken prion tandem repeats adopt a different structure than do the

mammalian prion tandem repeats.

The production of two mutually exclusive fragment patterns by proteinase K also has implications for the structure of the tandem repeats. The major 9 kDa fragment roughly matches the 9 kDa tryptic fragment. Producing the two 6.6 kDa fragments requires a cut in the middle of the 9 kDa fragment before its ends have been trimmed. These mutually exclusive cutting patterns may indicate that two ChPrPH6 conformations exist. Alternatively, occasional cutting between amino acids 80 and 110 may allow the 6.6 kDa fragments generated to subsequently adopt a new protease-resistant fold.

We have also investigated the chicken prion tandem repeat structure indirectly by assaying copper binding. Synthetic peptides composed of three or four of the ChPrP repeats bind copper in solution with low micromolar affinity. In mass spectrometry, a nested set of peaks appear that correspond to 0–4 copper atoms bound per 4 repeat peptide (11). Copper binding causes an apparent increase in the random coil content (12), an effect opposite of the helix formation observed using synthetic mammalian repeats (13). However, we do not observe copper binding by the mature, folded chicken prion. These data imply either (1) that the tandem amino acid repeats of ChPrPH6 have a different conformation than that of the synthetic peptides or (2) that copper binding is blocked by the rest of the chicken prion protein, e.g., by burying competent copper binding sites within the protein. A consequence of this model is that copper should destabilize ChPrPH6: as the protein unfolds, constraints on the conformation of the tandem repeats are lifted, and the protein amino terminus should become free to bind copper. In fact, 80  $\mu$ M copper lowered the melting temperature of ChPrPH6 by 30 °C, strongly destabilizing the prion protein. Table 2 summarizes the evidence that the avian repeats, unlike the mammalian repeats, form a well-folded domain. We can speculate that avian repeats evolved to maintain a folded form independent of a cofactor, and that mammalian repeats require a cofactor—copper or another molecule—to maintain a stable structure. The physiological implication is that copper binding is not the primary function of the prion protein.

Normal cellular processing of ChPrP has been extensively studied by Harris et al. (25), who observed a cleavage of ChPrP after amino acid 116 of ChPrP on the surface of ChPrP-expressing mouse neuroblastoma cells. The cleavage released a 10 kDa fragment (residues 25–116) into the extracellular matrix. In humans, a carboxy-terminal PrP<sup>C</sup> fragment beginning at H111 or M112 can be found both in healthy brains and in brains of patients with Creutzfeldt–Jakob disease (33). The cleavage of recombinant mPrP 23–231 between residues 118 and 119 (18) mirrors the observations of physiological cleavage of chicken prion and human prion, summarized in Figure 11. That the protease-resistant 9 kDa ChPrPH6 domain coincides with this region is most likely not coincidental. It has been suggested that soluble amino-terminal fragments might fulfill a biological role (26). This view is supported by our observation that the amino terminus forms a protease-resistant domain that exists as a stable, independent unit. The recent hypothesis that the prion protein C-terminal domain is related to signal peptidases (34) even raises the possibility that the prion N-terminal domain could be released under certain conditions by an autocatalytic C-terminal domain.

## ACKNOWLEDGMENT

We thank Darlene Groth, Ingrid Mehlhorn, Glenn Telling, and Stanley Prusiner for helpful advice and for supplying the chicken prion cDNA clone, Ralf Landgraf for protein refolding advice, and Danny Rice for initially coding the tryptic fragment analysis. The UCLA Protein Microsequencing Facility, aided by an NCI Cancer Support Center Grant, performed amino-terminal sequencing and analyses of amino acid content.

## REFERENCES

- Bolton, D. C., McKinley, M. P., and Prusiner, S. B. (1984) *Biochemistry* 23, 5898–5906.
- McKinley, M. P., Bolton, D. C., and Prusiner, S. B. (1983) *Cell* 35, 57–62.
- Brandner, S., Isenmann, I., Raeber, A., Fischer, M., Sailer, A., Kobayashi, Y., Marino, S., Weissmann, C., and Aguzzi, A. (1996) *Nature* 379, 339–343.
- Pan, K.-M., Baldwin, M., Nguyen, J., Gasset, M., Serban, A., Groth, D., Mehlhorn, I., Huang, Z., Fletterick, R. J., Cohen, F. E., and Prusiner, S. B. (1993) *Proc. Natl. Acad. Sci. U.S.A.* 90, 10962–10966.
- Caughey, B. W., Dong, A., Bhat, K. S., Ernst, D., Hayes, S. F., and Caughey, W. S. (1991) *Biochemistry* 30, 7672–7680.
- Merz, P. A., Somerville, R. A., Wisniewski, H. M., and Iqbal, K. (1981) *Acta Neuropathol.* 54, 63–74.
- Diringer, H., Gelderblom, H., Hilmert, H., Ozel, M., Edelbluth, C., and Kimberlin, R. H. (1983) *Nature* 306, 476–478.
- Prusiner, S. B., McKinley, M. P., Bowman, K. A., Bendheim, P. E., Bolton, D. C., Groth, D. F., and Glenner, G. G. (1983) *Cell* 35, 349–358.
- Stahl, N., Borchelt, D. R., Hsiao, K., and Prusiner, S. B. (1987) *Cell* 51, 229–240.
- Brown, D. R., Qin, K., Herms, J. W., Madlung, A., Manson, J., Strome, R., Fraser, P. E., Kruck, T., von Bohlen, A., Schulz-Schaeffer, W., Giese, A., Westaway, D., and Kretschmar, H. (1997) *Nature* 390, 684–687.
- Hornshaw, M. P., McDermott, J. R., and Candy, J. M. (1995) *Biochem. Biophys. Res. Commun.* 207, 621–629.
- Hornshaw, M. P., McDermott, J. R., Candy, J. M., and Lakey, J. H. (1995) *Biochem. Biophys. Res. Commun.* 214, 993–999.
- Miura, T., Hori-I, A., and Takeuchi, H. (1996) *FEBS Lett.* 396, 248–252.
- Tobler, I., Gaus, S. E., Deboer, T., Achermann, P., Fischer, M., Rüllicke, T., Moser, M., Oesch, B., McBride, P. A., and Manson, J. C. (1996) *Nature* 380, 639–642.
- Sakaguchi, S., Katamine, S., Nishida, N., Moriuchi, R., Shigematsu, K., Sugimoto, T., Nakatani, A., Kataoka, Y., Houtani, T., Shirabe, S., Okada, H., Hasegawa, S., Miyamoto, T., and Noda, T. (1996) *Nature* 380, 528–531.
- Collinge, J., Whittington, M. A., Sidle, K. C. L., Smith, C. J., Palmer, M. S., Clarke, A. R., and Jeffreys, J. G. R. (1994) *Nature* 370, 295–297.
- Pergami, P., Jaffe, H., and Safar, J. (1996) *Anal. Biochem.* 236, 63–73.
- Hornemann, S., Korth, C., Oesch, B., Riek, R., Wider, G., Wüthrich, K., and Glockshuber, R. (1997) *FEBS Lett.* 413, 277–281.
- Mehlhorn, I., Groth, D., Stöckel, J., Moffat, B., Reilly, D., Yansura, D., Willett, W. S., Baldwin, M., Fletterick, R., Cohen, F. E., Vandlen, R., Henner, D., and Prusiner, S. B. (1996) *Biochemistry* 35, 5528–5537.
- Riek, R., Hornemann, S., Wider, G., Glockshuber, R., and Wüthrich, K. (1997) *FEBS Lett.* 413, 282–288.
- Donne, D. G., Viles, J. H., Groth, D., Mehlhorn, I., James, T. L., Cohen, F. E., Prusiner, S. B., Wright, P. E., and Dyson, H. J. (1997) *Proc. Natl. Acad. Sci. U.S.A.* 94, 13452–13457.
- Harris, D. A., Falls, D. L., Johnson, F. A., and Fischbach, G. D. (1991) *Proc. Natl. Acad. Sci. U.S.A.* 88, 7664–7668.
- Schätzl, H. M., Da Costa, M., Taylor, L., Cohen, F. E., and Prusiner, S. B. (1995) *J. Mol. Biol.* 245, 362–374.

24. Endo, T., Groth, D., Prusiner, S. B., and Kobata, A. (1989) *Biochemistry* 28, 8380–8388.
25. Harris, D. A., Huber, M. T., van Dijken, P., Shyng, S.-L., Chait, B. T., and Wang, R. (1993) *Biochemistry* 32, 1009–1016.
26. Harris, D. A., Gorodinsky, A., Lehmann, S., Moulder, K., and Shyng, S.-L. (1996) *Curr. Top. Microbiol. Immunol.* 207, 77–93.
27. Georgiou, G. (1996) in *Protein Engineering: Principles and Practice* (Cleland, J. L., and Craik, C. S., Eds.) pp 101–127, Wiley-Liss, New York.
28. Andrade, M. A., Chacon, P., Merelo, J. J., and Moran, F. (1993) *Protein Eng.* 6, 383–390.
29. Thompson, J. D., Higgins, D. G., and Gibson, T. J. (1994) *Nucleic Acids Res.* 22, 4673–4680.
30. Liu, Y., Hart, P. J., Schlunegger, M. P., and Eisenberg, D. (1998) *Proc. Natl. Acad. Sci. U.S.A.* 95, 3437–3442.
31. Schlunegger, M. P., Bennett, M. J., and Eisenberg, D. (1997) *Adv. Protein Chem.* 50, 61–122.
32. Rost, B., Schneider, R., and Sander, C. (1994) *CABIOS* 10, 53–60.
33. Chen, S. G., Teplow, D. B., Parchi, P., Teller, J. K., Gambetti, P., and Autilio-Gambetti, L. (1995) *J. Biol. Chem.* 270, 19173–19180.
34. Glockshuber, R., Hornemann, S., Billeter, M., Riek, R., Wider, G., and Wüthrich, K. (1998) *FEBS Lett.* 426, 291–296.
35. Weiss, S., Famulok, M., Edenhofer, F., Wang, Y.-H., Jones, I. M., Groschup, M., and Winnacker, E.-L. (1995) *J. Virol.* 69, 4776–4783.
36. This work.

BI981487F